https://doi.org/10.33271/nvngu/2024-3/072

I. F. Alrefo*[1],
orcid.org/0000-0002-5626-7121,
M. O. Rawashdeh[1],
orcid.org/0000-0001-7241-5000,
O. Matsulevych[2],
orcid.org/0000-0001-5553-709X,
O. Vershkov[2],
orcid.org/0000-0001-5137-3235,
S. Halko[2],
orcid.org/0000-0001-7991-0311,
O. Suprun[2],
orcid.org/0000-0003-4369-712X

1 – Al-Balqa Applied University, Amman, Jordan
2 – Dmytro Motornyi Tavria State Agrotechnological University, Melitopol, Ukraine
* Corresponding author e-mail: ibrhem@bau.edu.jo

DESIGNING THE FUNCTIONAL SURFACES OF CAMSHAFT CAMS OF INTERNAL COMBUSTION ENGINES

Purpose. Automation of the process of designing the profile of gas distribution mechanisms (GDM) of internal combustion engines of all types, ensuring the reliability and durability of their operation.

Methodology. The speed and acceleration of the GDM pusher were determined by applying discrete differentiation. This enabled forming a differential band of values of the first and second separated differences of the original coordinates of the pusher's movement schedule on the basis of which the average speed and acceleration graphs of the GDM pusher were constructed. The SolidWorks CAD system was used to automate computer simulation of the cams' functional surfaces to obtain a 3D model of the camshaft, which can provide the required accuracy.

Findings. In order to form plane contours of the GDM functional surfaces of internal combustion engines, which are given with the necessary accuracy, the authors propose algorithms for obtaining linear elements of computer models of the projected surfaces. The proposed method was tested using CAD to optimize the geometric shape of the cam to obtain a computer model of the camshaft in order to increase the performance of the GDM of the internal combustion engine.

Originality. The original method is provided for determining the values of speeds and accelerations of the GDM pusher's motions of internal combustion engine, which is based on constructing a band of differential projections of the first and second separated differences of the values of its movement coordinates. This method ensures the absence of oscillation of the obtained speed and acceleration graphs of the pusher's movement by determining the values at the beginning and end points of the graph, which was not possible by using the traditional method.

Practical value. The methodology of automated design of the working surfaces of distribution shafts of all types with ensuring reliability and durability of their operation has been developed.

Keywords: *internal combustion engine, distribution shaft, pusher, cam, discrete differentiation, separated differences*

Introduction. The camshaft of the internal combustion engine (ICE) is responsible for opening and closing the inlet and release valves, that is, for gas distribution directly in the combustion chamber of the engine. The design features of the engine and the camshaft itself, as well as the correct adjustment of the gas distribution mechanism (GDM), depend on the efficiency of the engine: power, dynamics, efficiency.

Its operation enables synchronization of engine cycles of fuel-air mixture and exhaust gas inlet and release.

The construction of the camshaft changes in shape while retaining its functionality, and the camshaft remains a constant part of the ICE.

The camshaft is an extremely wear-resistant part that can last the vehicle's entire service life. However, there are situations when the camshaft fails, which can lead to negative consequences. This happens for the following reasons:

1. Aggressive driving – active manoeuvring, sharp braking and dynamic acceleration.

2. Low oil level, which increases the wear on the movable components of the ICE including the camshaft.

3. Using poor-quality oil – the presence of abrasive particles in the working fluid leaves damage on the surface, resulting in accelerated wear of camshaft cams.

4. Vibration of the cam/pusher system.

When operating, the ICE is heated to high temperatures, causing parts to increase in size. Bearing this in mind, engineers provide a thermal gap designed to increase the size. If this gap is adjusted incorrectly, the cam will hit the valve tappet instead of pressing it.

Another factor in ensuring the smooth operation of the GDM, including the camshaft, directly depends on the quality of lubrication of their working surfaces. The main criterion of the surface lubrication quality is the continuity of its supply to the working surfaces of the engine.

Oil shortage can cause the parts to overheat, which causes the metal to distort and entails breakage of the adjacent parts of the ICE (sheave, chain or GDM belt).

The vibration that occurs when the cam and the pusher interact is caused by the interrupted lubrication between their surfaces and by the cam surface damage.

One of the factors in ensuring reliable engine operation is the uninterrupted supply of lubrication to the working surfaces of the camshaft. This can be achieved by improving the geometry of the working surface of the cam.

Literature review. Cyclic impact loads on the surface of the cam and the pusher often cause premature wear of the cam profile and affect the camshaft rotation speed, valve movement and torque. Also, in cyclic bending and torsion, fatigue failure of the camshaft occurs when loads are concentrated. This requires the camshaft to be not only wear-resistant, but also to have sufficient impact resistance [1, 2].

Solidworks and ANSYS 17.0 software for simulation based on finite element method (FEM-simulation) was used in [3] to investigate the breakdown causes of a specific ICE camshaft on Kijang LGX. The analysis of the test results showed that the camshaft breakdown occurred due to extreme temperature differences in the transition zones, which potentially affects the

formation and spread of cracks and reduced load capacity of the camshaft.

Special attention is paid to the study of causes of failures of camshafts manufactured using the hydroforming technology (HFT) of pipes and ways of their elimination.

The difficulty in operating these prefabricated camshafts is due to the fact that the profile cam is the assembly unit when connected to the hollow shaft (tube) under hydraulic pressure. Experiments with orthogonal torsion and laser measurements have revealed the main causes of camshaft failure.

In [4, 5], methods for estimating the quality of assembled camshafts manufactured using the pulsating HFT are discussed. The novelty of the design of such camshafts consists in applying a pulsating hydraulic pressure to the inner part of the hollow shaft so that, after deformation under pressure, it provides a cam-strapping fit (cam holes of non-circular structure). It has been determined that the camshaft quality depends on the pulsation amplitude, pulsation frequency and hydraulic pressure as well as the quality of the working surfaces. The obtained research results lead to the conclusion that the camshafts assembled using pulsating HFT are more difficult to manufacture than the camshafts produced by casting or stamping. In addition, the reliability of such shafts is dubious [6].

One of the primary causes of camshaft failure is insufficient cam/pusher lubrication and poor cam surface condition. Thus, in the best case, vibrations, impacts, etc. occur, which affects the stability of the cam mechanism. In the worst case, this results in the separation of the cam and shaft, resulting in the failure of the camshaft [7].

The accuracy of camshaft cams plays an important role in the reliable operation of the GDM. The stability of the entire ICE depends on their reliable and uninterrupted operation.

The authors of [8, 9] examine the influence of the accuracy of manufacturing rotor functional surfaces on the reliability of the operation of hydraulic positive-displacement machines.

The article develops a calculation scheme, as well as the geometric and functional relationship of location of contact points of hydraulic motor rotor profiles and control methods for error of shape of internal and external rotors of the hydraulic motor. This method can be applied to determine the gap between the working surfaces of the ICE cam mechanisms. This gap can be used as a parameter for determining the technical state of the cam mechanism, and its limit value can be used as a basis for normalizing the functional parameters that determine the performance of the ICE. However, fluctuations in the shape of the cam work surfaces are chaotic and cyclical and have a significant impact on the change in the maximum allowable gap.

A new approach to designing the cam profile for the development of a high-performance new class ICE is described in [10]. The recuperated split cycle engine (RSCE) has unique requirements for valve lift, duration and phasing compared to the conventional 4-stroke engine.

But to ensure the high efficiency of such an engine, an increased control of the release valve opening is necessary, which can only be achieved by the high-quality design and manufacture of camshaft cam surfaces. In [10] requirements for cam profile, functions, design, analysis and test results of heavy engine with recovery and separated cycle are presented. For light- and middle-class engines, this method requires improvement and adjustments to the working conditions. Particular attention should be paid to the curvilinear surfaces of the cams of the ICE camshaft, which can provide the required opening and closing quality of the engine valves.

A new conceptual cam for infinitely variable adjustment of gas distribution phases is proposed by the authors of [11, 12]. A series of experiments with 13 camshafts with the same curvilinear cam surface and different distribution angles was carried out and processed. Based on the synthesis and processing of the experiment results, it was determined that the cam with the calculated profile provides the necessary characteristics of the gas exchange process in the engine. But, at the same time, more rapid wear was observed, both on the flat and hemispherical tips of the pusher.

Such problems are usually caused by insufficient lubrication of the working (functional) surfaces of the machinery. This applies not only to ICE gas distribution mechanisms but also to other mechanisms of this type. For example, the analysis of the design and operation of the rotary-planetary mechanism [12] revealed a major lack of its operation reliability, specifically the jamming caused by a self-induced vortex of reverse dry friction when the rotor/stator system interacts. It is proposed to correct this deficiency by improving the geometry of the rotor and stator working surfaces.

Similar approach to elimination of defects can be applied to other mechanisms [13, 14]. For example, to gas distribution mechanisms of the engine.

While preparing the article, it became necessary to analyse the dynamic behaviour of the cam pusher system for different values of valve lifting and operating speeds and accelerations. In [15], the research was carried out using methods of analysis in temporal and frequency domains. Two cases were tested for maximum valve lifts with appropriate operating speeds. It has been observed that with the increase in the pusher working speed, the value of the displacement amplitude increases. However, an increase in the probability of the pusher-cam system failure due to insufficient lubrication of the working surfaces was also observed [15].

The valve lift design of the cam pusher system is very important for improving the dynamic characteristics of the ICE. Potential problems due to inadvertent vibrations in the high-speed engine are the jump of the pusher, and the contact surface of the valves and the seat, which cause collision in the pusher-cam system. The degree of collision depends on the valve lift and valve closing speed. When the cam and the pusher collide, great forces and tensions arise. This can lead to premature system failure due to unwanted vibration. Another problem is that the rotation speed of the camshaft is not constant in the case of continuous operation of the ICE.

Purpose of the article. The aim of the paper is to develop a universal method for designing working profiles of cam mechanisms of ICE of heavy, medium and light types.

To achieve this aim, it is necessary to solve the following tasks:

1. To analyse the calculation method of cam profile used in engine building.

2. To identify the deficiencies of the traditional methodology.

3. To propose a method for obtaining the coordinates of the working profile of the camshaft cam of the ICE based on discrete differentiation of the tabular function.

Methods. The main structural elements of the camshaft (Fig. 1) are cams, which open the valves directly or via pushers. The supporting elements (necks) are mounted in sliding bearings (inserts) on which the camshaft rotates due to the oil wedge effect with minimal friction.

Consider cam profiling of the GDM for the ICE. The cam profile of the valve DGM is set in the polar coordinate system,

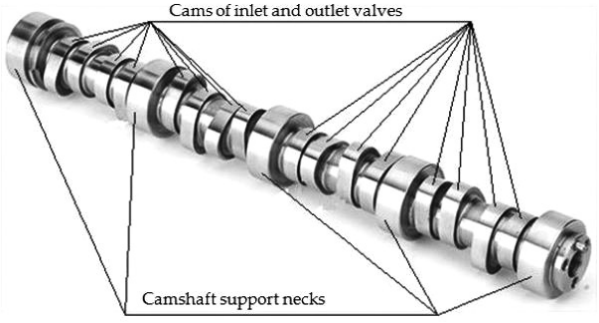

Fig. 1. Main structural elements of the camshaft

the centre of which belongs to the camshaft rotation axis. The plane of assignment is perpendicular to the shaft axis. Each i^{th} point of the cam profile has α_i coordinates (cam angle from the polar axis passing through the highest point of the profile) and ρi coordinates (polar radius).

The main task of cam profiling is to determine the coordinates of the polar radius ρ_i and the rotation angle of the cam α_i of its points, depending on the pusher's motion law. This law determines the movement of the valve, which provides a preset opening time-section and a change in the working medium in the engine cylinder. Thus, the pusher's motion law is determined by the thermodynamic calculation of the processes in the ICE cylinder [16, 17].

At this stage of profiling, it is considered to be specified in the form of the table of movements of the pusher S through the cam rotation angle α.

At present, many design schemes of motion transfer from the cam to the pusher have been proposed. The most common one is when the axis of the pusher passes through the centre of rotation of the cam, and the disc of the pusher is perpendicular to its axis and has a flat shape (Fig. 2). When profiling, the rotational motion of the pusher plate around the axis is not taken into account. The method adopted in engine building for calculating the cam profile, as well as its manufacturing by milling and subsequent grinding, does not require other data than the pusher's motion law. It is assumed that the angular speed ω of the camshaft is constant (arbitrarily accepted in calculations as non-negative) [16].

As can be seen from Fig. 2, the position of the pusher plate relative to the camshaft axis is determined by the distance S

$$S = \rho_0 + s,$$

where ρ_0 is the radius of the cam occiput (appointed from constructive, technological durability, etc. considerations); s – pusher lift at a specific point in time.

The kinematic analysis of the mechanism determines the following parameters.

The sliding speed of the pusher on the cam υ_{sl}

$$\upsilon_{sl} = S \cdot \omega,$$

where ω is angular cam rotation speed;

$$\omega = \frac{\pi \cdot n}{30},$$

where n is camshaft rotation speed, rev/min.

The speed of movement of the contact point on the pusher l_P° is

$$l_P^\circ = \frac{\overset{\circ\circ}{S}}{\omega} = s'' \cdot \omega, \qquad (1)$$

where $\overset{\circ\circ}{S}$ is the pusher's acceleration (second derivative of motion s through time t); s''– acceleration analogue (second derivative through cam rotation angle φ).

With the appropriate choice of the reference point, angle φ coincides with angle α, which determines the position of the cam and the pusher in the coordinate system associated with the cam. As a rule, the α angles are calculated through the radius-vector of the cam apex (Fig. 2).

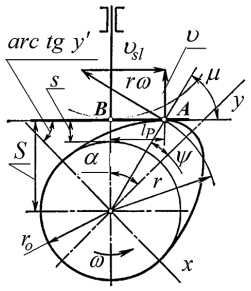

Fig. 2. Structural scheme of motion transfer from the cam to the pusher

The speed of the contact point on the cam profile l_C°

$$l_C^\circ = l_P^\circ + \upsilon_{sl} = \left(S + \frac{d^2 S}{d\alpha^2} \right) \cdot \omega.$$

This speed is proportional to the curvature radius r of the cam profile at the contact point [16].

$$l_C^\circ = r \cdot \omega.$$

Then

$$r = \rho_0 + S + s''. \qquad (2)$$

The coefficient of the specific slide of the cam and the pusher, respectively, is found as the ratio of slip velocity υ_{sl} to the velocity of the contact point

$$\lambda_C = \frac{\upsilon_{sl}}{l_C^\circ - \dfrac{S}{r}};$$

$$\lambda_P = \frac{\upsilon_{sl}}{l_P^\circ - \dfrac{S}{s''}}.$$

These coefficients characterize the heat intensity and wear of the conjugate surfaces.

Hydrodynamic efficient speed υ_H in conjunction with characterizing the conditions under which the oil wedge is formed

$$\upsilon_H = l_C^\circ + l_P^\circ = (r + s'') \cdot \omega.$$

The faster the module of the speed υ_H, the better the conditions for oil wedge formation, the less wear of the pusher-cam system.

When designing the cam, attention is drawn to the fact that in the position where the acceleration of the pusher is equal to zero (at the beginning and end of the valve lift and at the point of change of the acceleration sign) the coefficient λ_P increases indefinitely (1), hence increases the thermal tension of the connection. Therefore, it is not desirable to have an area of constant pusher lift the at the top of the cam in the cam profile. A cam profile as an arc of an involute circle is also undesirable, because the speed of the pusher is constant, and the acceleration is zero.

The ratio υ_H/ω in the negative acceleration section of the pusher is much smaller than in the positive acceleration section, since the curvature radius in the first case is much smaller (2). Therefore, the conditions for keeping the oil wedge in the first case are significantly worsened, and at $\upsilon_H/\omega = 0$ – non-existent.

The filling of the cylinder is determined by the area F under the curve of the pusher on the rotation angle of the cam. It was proved in [18] that

$$F = L - 2\pi \cdot \rho_0,$$

where L is the full length of the cam contour.

When analysing the pusher's motion law, the coordinates x and y of the cam profile points are determined by the formulas

$$x = S \cdot \sin\varphi + s' \cos\varphi: \quad y = S \cdot \cos\varphi - s' \sin\varphi,$$

or at polar coordinates

$$\rho = \sqrt{S^2 + s'^2}; \quad \psi = \varphi + \operatorname{arctg}\frac{s'}{S}. \qquad (3)$$

The coordinates R_W and β_W (Fig. 3) of the centre of the grinding wheel for cam profile processing, respectively, are equal

$$R_W = (S + r_W)/\cos\zeta_W;$$

$$\beta_C = \alpha + \zeta_W;$$

$$\zeta_W = \psi - \alpha,$$

where r_W is the radius of the grinding wheel, (Fig. 3).

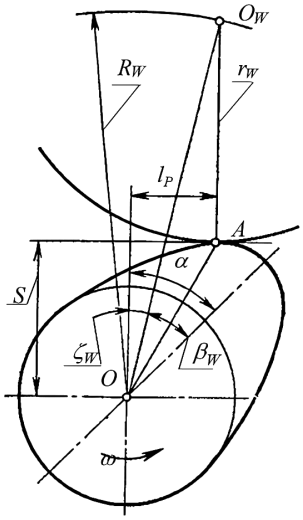

Fig. 3. Coordinates R_W and β_W of the center of the grinding wheel for cam profile processing

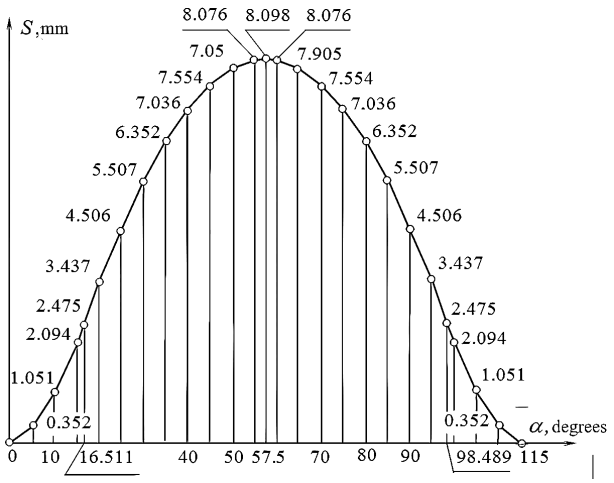

Fig. 4. Motion graph of the diesel engine pusher

If the pusher's motion law is presented graphically by some curve [18, 19], graphical differentiation of this curve shall be used for calculations [20].

In the tabular presentation of the pusher's motion law, numerical differentiation of the tabular function is used if the table of the pusher's lift is specified with an accuracy greater than the accuracy of the cam profile manufacturing and control.

$$s_i' \approx (S_{i+1} - S_{i-1})/2 \cdot \Delta\alpha;$$

$$s_i'' \approx (S_{i+1} - 2S_i + S_{i-1})/\Delta\alpha^2,$$

where $\Delta\alpha$ is an argument step on a uniform grid of α_i angles.

Otherwise, numerical differentiation is used, with preliminary smoothing of the original data, aggravated by rounding errors that occurred when compiling the Table. In particular, the formulas from [16] may be applied.

$$s_i' \approx [2(S_{i+2} - S_{i-2}) + S_{i+1} - S_{i-1}]/10 \cdot \Delta\alpha; \quad (4)$$

$$s_i'' \approx \left[\begin{matrix} 4(S_{i+4} + S_{i+3} - S_{i+1} - S_{i-1} + S_{i-3} + S_{i-4}) \\ +S_{i+2} - S_{i-2} - 10S_i \end{matrix}\right] \Big/ 100 \cdot \Delta\alpha^2. \quad (5)$$

However, this method for defining derivative analogues has significant disadvantages:

1. Calculated values of s_i' and s_i'' are highly dependent on the rounding errors in the Table.

2. The more the table of the values is adjusted, the more the pusher's law is distorted.

Thus, the methods of discrete differentiation of the tabular function have greater reliability.

Results. Consider the solution of this problem using the example of the motion graph of the diesel engine pusher (Fig. 4).

The graph is a symmetric relative to $\alpha = 57°30'$ discretely represented curve with the step of the base grid of $\Delta\alpha = 5°$. It is obvious that, according to the above, the calculation of s_i' and s_i'' should be done by formulas (4 and 5). The data of these calculations are shown in Table 1.

As can be seen from Table 1, the proposed method for determining the speeds s_i' and the accelerations s_i'' of the pusher does not involve determining their values at the starting and end points impossible.

The present article offers a method for determining the speeds s_i' and the accelerations s_i'' of the pusher's movement based on the construction of the band of differential projections on the basis of the 1^{st} and 2^{nd} separated differences of values of $S_i(\alpha)$. The speed s_i' and acceleration s_i'' values arranged

Table 1

Data of calculations s_i' and s_i''

No.	α	S_i	s_i'	s_i''	No.	α	S_i	s_i'	s_i''
1	0	0	–	–	15	60	8.076	–0.01746	–0.00693
2	5	0.352	–	–	16	65	7.905	–0.05204	–0.00687
3	10	1.051	0.17376	–	17	70	7.554	–0.08634	–0.00676
4	15	2.094	0.2146	–	18	75	7.036	–0.11996	–0.00642
5	16.511	2.475	–	–	19	80	6.352	–0.1525	–0.00618
6	20	3.473	0.22648	0.000155	20	85	5.507	–0.17944	–0.00543
7	25	4.506	0.211	–0.00342	21	90	4.506	–0.211	–0.00342
8	30	5.507	0.17944	–0.00543	22	95	3.473	–0.22648	0.000155
9	35	6.352	0.1525	–0.00618	23	98.489	2.475	–	–
10	40	7.036	0.11996	–0.00642	24	100	2.094	–0.2146	–
11	45	7.554	0.08634	–0.00676	25	105	1.051	–0.17376	–
12	50	7.905	0.05204	–0.00687	26	110	0.357	–	–
13	55	8.076	0.01746	–0.00693	27	115	0	–	–
14	57.5	8.098	0	–	–	–	–	–	–

within the resulting band can ensure that the solution does not oscillate [20].

The set of values of the first approximation according to the proposed methodology [21, 22] is given in Table 2 in column 6. Composite smoothing with discretely represented reference curves is applied to this set to obtain a non-sampling discretely represented curve of values of s_i', since the oscillation of the graph of the I^{st} derivative will lead to oscillation of the values of ρ and ψ from (3) and, consequently, to the oscillation of the theoretical cam profile [23, 24]. The smoothed values of s_i' and s_i'' are presented in column 7 of Table 2, and the corresponding points [25], as well as the points of column 4, are inscribed in a band of the1st separated differences (Fig. 5).

The final values of S_i should be clarified based on the analysis of the process in the cylinder (dynamics of valve opening, time-section, etc.).

We shall consider that such adjustments have been made, and new ordinates of the adjusted points of the motion graph as well as the adjusted values of the I^{st} derivative are presented in Table 2.

To calculate the acceleration analogue (the second derivative of s_i'') in the traditional way we use (5) for the corrected discretely represented curve S_i. The results are presented in Table 2 (column 8).

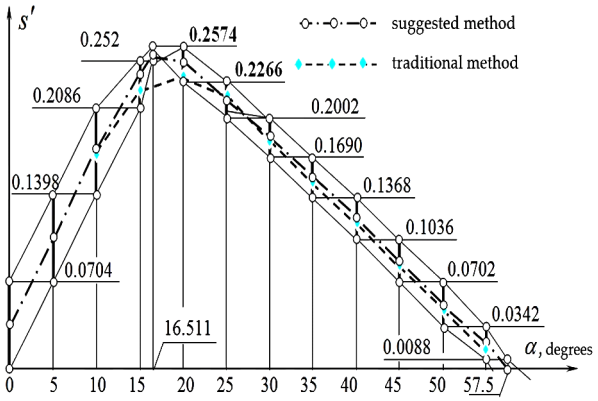

Fig. 5. Graph of dependence of values of s_i' on α

The calculation of the proposed method is based on a discretely presented curve based on Fig. 5 according to the approximation for the corrected values of S_i. Fig. 6 presents a graph of dependence of s_i' values on the values of α calculated according to both the traditional method and the proposed one.

For the points of this graph, once again we calculate I^{st} separated differences and construct a differential band of val-

Table 2

Data of smoothed values s_i' and s_i''

No.	α	S_i	Traditional method		First approximation of s_i'	Smoothed value of s_i'	First approximation of $s_i'' \cdot 10^{-2}$	Smoothed value of $s_i'' \cdot 10^{-2}$
			s_i'	$s_i'' \cdot 10^{-2}$				
1	2	3	4	5	6	7	8	9
1	0	0	–	–	0.0357	0.0357	1.4339	1.4339
2	5	0.352	–	–	0.1051	0.1051	1.385	1.385
3	10	1.051	0.16976	–	0.1742	0.1742	1.2872	1.2872
4	15	2.094	0.2126	–	0.2303	0.23382	1.19249	1.1925
5	16.51	2.475	–	–	0.2547	0.25184	0.40099	0.40099
6	20	3.373	0.22648	0.0555	0.242	0.238212	–0.4813	–0.481
7	25	4.506	0.213	–0.326	0.2134	0.209612	–0.574	–0.574
8	30	5.507	0.18344	–0.547	0.1846	0.180812	–0.605	–0.622
9	35	6.352	0.1525	–0.634	0.1529	0.149112	–0.62997	–0.641
10	40	7.036	0.11996	–0.658	0.1202	0.117815	–0.63074	–0.659
11	45	7.554	0.08634	–0.676	0.0869	0.086038	–0.66352	–0.676
12	50	7.905	0.05204	–0.687	0.0522	0.051463	–0.68326	–0.688
13	55	8.076	0.01746	–0.693	0.0215	0.017712	–0.69175	–0.702
14	57.5	8.098	0	–	0	0	–0.70848	–0.706
15	60	8.076	–0.01746	–0.693	–0.0215	–0.01771	–0.69175	–0.702
16	65	7.905	–0.05204	–0.687	–0.0522	–0.051463	–0.68326	–0.688
17	70	7.554	–0.08634	–0.676	–0.0869	–0.086038	–0.66352	–0.676
18	75	7.036	–0.11996	–0.658	–0.1202	–0.117815	–0.63074	–0.659
19	80	6.352	–0.1525	–0.634	–0.1529	–0.149112	–0.62997	–0.641
20	85	5.507	–0.18344	–0.547	–0.1846	–0.180812	–0.605	–0.622
21	90	4.506	–0.213	–0.326	–0.2134	–0.209612	–0.574	–0.574
22	95	3.373	–0.22648	0.0555	–0.242	–0.238212	–0.4813	–0.481
23	98.48	2.475	–	–	–0.2547	–0.25184	0.40099	0.401
24	100	2.094	–0.2126	–	–0.2303	–0.23382	1.19249	1.1925
25	105	1.051	–0.16976	–	–0.1742	–0.1742	1.2872	1.2872
26	110	0.352	–	–	–0.1051	–0.1051	1.385	1.385
27	115	0	–	–	–0.0357	–0.0357	1.4339	1.4339

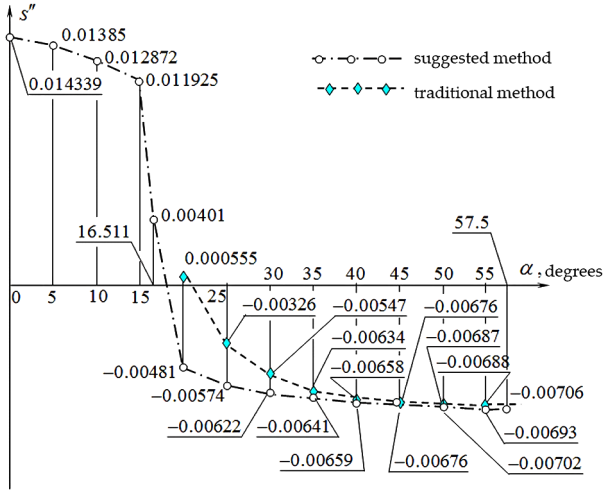

Fig. 6. Graph of dependence of values of s_i'' on α

ues of s_i'' through α, and Fig. 6 presents comparative acceleration schedules of the pusher, calculated traditionally and using the proposed method. The values obtained, smoothed according to the proposed methodology, are presented in Table 2 (column 9).

Conclusion. The analysis of the publications revealed that cyclic impacts on the surface of the cam and pusher caused premature wear of the cam profile and affected camshaft rotation, valve movement and torque. The jump of the pusher upon contact of the surfaces of the valve and seat causes collision in the pusher-cam system. This leads to the destruction of the cam's working surface.

In order to solve the problem of geometric modelling of the working surfaces of cam mechanisms, the analysis of the accepted (traditional) calculation method of the cam profile has been carried out, and its deficiencies have been revealed.

The traditional method for determining derivative analogues has significant disadvantages – the calculation values of the analogues of speeds s_i' and acceleration s_i'' of the pusher's motion are highly dependent on the rounding errors in the Table.

The article offers a universal method for designing working profiles of cam mechanisms of the ICE, specifically by obtaining the cam profile surface coordinates of the camshaft of the ICE on the basis of discrete differentiation of the tabular function.

The speed and acceleration graphs of the pusher, constructed by the proposed method, are of non-oscillating character, with a smoother change of the indicators and fully correspond to the motion graphs of S_i.

Using the obtained data, it is possible to calculate the parameters that determine the kinematic analysis of the GDM of the input data: φ_i – cam angle; S_i – the distance of the cam axis from the pusher plate; s_i' – pusher speed; s_i'' – pusher acceleration.

By comparing the values of s_i' and s_i'' obtained using the traditional method and the proposed one, we can state the following:

1. The smoothed values of s_i' and s_i'' are located inside the band (unlike the traditional ones), which indicates that there is no oscillation.

2. The proposed methodology enables obtaining the values of s_i' and s_i'' at all points as opposed to the traditional method, which does not have the required values at the first and last four points.

Discretely presented curves of values of s_i' and s_i'' have better dynamics of passage of points where the acceleration of the pusher is equal to zero (points of change of acceleration sign) in which the thermal tension of the connection increases significantly.

References.

1. Mahat, A. H. B., Saleh, M. H. B., & Fauthan, M. A. B. (2018). Malaysia Investigation and Failure Analysis for Camshaft. *Advanced Journal of Technical and Vocational Education, 2*(3), 23-27. https://doi.org/10.26666/rmp.ajtve.2018.3.4.

2. Prasetya, R., & Kijang, A. (2021). LGX camshaft's failure analysis using the finite element method approach. *IOP Conference Series: Materials Science and Engineering, 1034*, 012014. https://doi.org/10.1088/1757-899X/1034/1/012014.

3. Ma, J. P., Yang, L. F., Liu, J., Chen, Z. B., & He, Y. L. (2021). Evaluating the Quality of Assembled Camshafts under Pulsating Hydroforming. *Journal of Manufacturing Processes, 61*, 69-82.

4. Ma, J. P., Yang, L. F., Huang, J. J., Chen, Z. B., He, Y. L., & Jiang, J. Y. (2021). Residual Contact Pressure and Elastic Recovery of an Assembled Camshaft using Tube Hydroforming. *CIRP Journal of Manufacturing Science and Technology, 32*, 287-298.

5. Gao, G. Y., Zhang, Z., Cai, C., Zhang, J. L., & Nie, B. H. (2019). Cavitation Damage Prediction of Stainless Steels Using an Artificial Neural Network Approach. *Metals, 9*, 506.

6. Qi, B., Sun, X. M., Liu, B. J., Wu, X., Gao, R. T., Zhu, H., & Li, Y. H. (2022). Influencing Factors of Agricultural Machinery Accidents Based on Fuzzy Fault Tree Analysis. *Journal of Computational Methods in Sciences and Engineering, 22*, 871-881.

7. Jianping, M., Lianfa, Y., Lin, S., Zhiwei, G., Saisai, P., & Haimei, H. (2022). Failure Analysis of Hydraulic Expanding Assembled Camshafts Using BP Neural Network and Failure Tree Theory. *Metals, 12*, 1639. https://doi.org/10.3390/met12101639.

8. Panchenko, A., Voloshina, A., Boltianska, N., Pashchenko, V., & Volkov, S. (2021). Manufacturing Error of the Toothed Profile of Rotors for an Orbital Hydraulic Motor. *In Advanced Manufacturing Processes III. Inter Partner. Lecture Notes in Mechanical Engineering,* (pp. 22-32). Springer: Cham. https://doi.org/10.1007/978-3-030-91327-4_3.

9. Panchenko, A., Voloshina, A., Milaeva, I., Panchenko, I., & Titova, O. (2018). The Influence of the form Error after Rotor Manufacturing on the Output Characteristics of an Orbital Hydraulic Motor. *International Journal of Engineering and Technology, 7*(4.3), 1-5. https://doi.org/10.14419/ijet.v7i4.3.19542.

10. Ortolani, P., & Nation, F. (2023). New Cam Profile Design Approach, Analysis and Testing for Extreme High Efficiency Internal Combustion Engine Development. *SAE Technical Paper, 01*(0436). https://doi.org/10.4271/2023-01-0436.

11. Sürmen, A., Arslan, R., Kopmaz, O., Avcı, A., Karagöz, İ., & Karamangil, M. İ. (2017). Development of a variable-profile cam to enhance the volumetric efficiency of IC engines. *International Journal Vehicle Design*, *73*, 1/2/3, 63-75.

12. Alrefo, I. F., Matsulevych, O., Vershkov, O., Halko, S., Suprun, O., & Miroshnyk, O. (2023). Designing the working surfaces of rotary planetary mechanisms. *Naukovyi Visnyk Natsionalnoho Hirnychoho Universytetu,* (4), 82-88. https://doi.org/10.33271/nvngu/2023-4/082.

13. Havrylenko, Y., Cortez, J. I., Kholodniak, Y., & Garcia, G. T. (2020). Modelling of surfaces of engineering products on the basis of array of points. *Tehnički vjesnik, 27*(6), 2034-2043. https://doi.org/10.17559/TV-20190720081227.

14. Havrylenko, Y., & Kholodniak, Y. (2014). Formation of geometric model of the impeller of the turbocharger. *Proceedings of the Tavria State Agrotechnological University, 14,* 48-53.

15. Sarıdemir, S., & Saruhan, H. (2014). Experimental analysis of maximum valve lift effects in cam-follower system for internal combustion engines. *Journal of Mechanical Science and Technology, 28*, 3443-3448.

16. Koliisnikova, T., Tatarchuk, O., Zaiats, H., Stadnyk, V., & Konovalenko, Y. (2019). Theoretical investigation of operating process of conrod-free model cylinder. *Bulletin of the Dnipro State Academy of Construction and Architecture, 4*, 255-256.

17. Slynko, G., Ryaboshapka, N., Sukhonos, R., Yevsyeyeva, N., & Soldatchenkov, O. (2024). Study of the influence of misfires on the uneven ro-tation of the crankshaft of a gasoline engine. *New materials and technologies in metallurgy and mechanical engineering, 1*, 82-88. https://doi.org/10.15588/1607-6885-2024-1-11.

18. Havrylenko, Y., Kholodniak, Y., Halko, S., Vershkov, O., Bondarenko, L., Suprun, O., ..., & Gackowska, M. (2021). Interpolation with specified error of a point series belonging to a monotone curve. *Entropy, 23*(5), 493, 1-13. https://doi.org/10.3390/e23050493.

19. Golovanevskiy, V., & Kondratiev, A. (2021). Elastic Properties of Steel-Cord Rubber Conveyor Belt. *Experimental Techniques, 45*(2), 217-226. https://doi.org/10.1007/s40799-021-00439-3.

20. Havrylenko, Y., Kholodniak, Y., Halko, S., Vershkov, O., Miroshnyk, O., Suprun, O., ..., & Śrutek, M. (2021). Representation of a monotone curve by a contour with regular change in curvature. *Entropy, 23*(7), 923, 1-14. https://doi.org/10.3390/e23070923.
21. Kondratiev, A., Gaidachuk, V., Nabokina, T., & Kovalenko, V. (2019). Determination of the influence of deflections in the thickness of a composite material on its physical and mechanical properties with a local damage to its wholeness. *Eastern-European Journal of Enterprise Technologies, 4*, 1(100), 6-13. https://doi.org/10.15587/1729-4061.2019.174025.
22. Kondratiev, A., & Gaidachuk, V. (2019). Weight-based optimization of sandwich shelled composite structures with a honeycomb filler. *Eastern-European Journal of Enterprise Technologies, 1*(97), 24-33. https://doi.org/10.15587/1729-4061.2019.154928.
23. Havrylenko, Y., Kholodniak, Y., Vershkov, O., & Naidysh, A. (2018). Development of the method for the formation of one-dimensional contours by the assigned interpolation accuracy. *Eastern-European Journal of Enterprise Technologies*, *1*(4(91), 76-82. https://doi.org/10.15587/1729-4061.2018.123921.
24. Argyros, I. K., & George, S. (2016). On the convergence of Newton-like methods using restricted domains. *Numerical Algorithms, 75*(3), 553-567. https://doi.org/10.1007/s11075-016-0211-y.
25. Liu, S., Chen, Z., & Zhu, Y. (2015). Rational Quadratic Trigonometric Interpolation Spline for Data Visualization. *Mathematical Problems in Engineering, 983120*, 1-20. https://doi.org/10.1155/2015/983120.

Проєктування функціональних поверхонь кулачків розподільчого валу двигунів внутрішнього згоряння

І. Ф. Альрефо[*1], *М. О. Равашдех*[1], *О. Є. Мацулевич*[2], *О. О. Вершков*[2], *С. В. Галько*[2], *О. М. Супрун*[2]

1 – Університет Ал-Балка, м. Аман, Йорданія
2 – Таврійський державний агротехнологічний університет імені Дмитра Моторного, м. Мелітополь, Україна
[*] Автор-кореспондент e-mail: ibrhem@bau.edu.jo

Мета. Автоматизація процесу проєктування профілю кулачків газорозподільних механізмів (ГРМ) двигунів внутрішнього згоряння всіх типів із забезпеченням надійності й довговічності їх роботи.

Методика. Визначення швидкості та прискорення переміщення штовхача ГРМ здійснювалося з використанням дискретного диференціювання. Це дало можливість забезпечити формування диференціальної смуги значень перших і других розділених різницевих координат графіка переміщення штовхача, на підставі яких були побудовані усереднені графіки швидкостей і прискорень штовхача ГРМ. Для автоматизації комп'ютерного моделювання функціональних поверхонь кулачків з отриманням тривимірної моделі розподільчого валу була використана CAD-система SolidWorks, що у змозі забезпечити необхідну точність.

Результати. Для формування плоских контурів функціональних поверхонь газорозподільних механізмів двигунів внутрішнього згоряння, які задані з необхідною точністю, авторами запропоновані алгоритми отримання лінійних елементів комп'ютерних моделей поверхонь, що проєктуються. Апробація запропонованої методики проведена з використанням САПР при оптимізації геометричної форми кулачка для отримання комп'ютерної моделі розподільного валу з метою збільшення продуктивності ГРМ двигуна внутрішнього згоряння.

Наукова новизна. Надана оригінальна методика визначення значень швидкостей і прискорень рухів штовхача газорозподільного механізму двигуна внутрішнього згоряння, що заснована на побудові смуги диференціальних проєкцій перших і других розділених різниць значень координат його переміщення. Дана методика дозволяє забезпечити відсутність осциляції отриманих графіків швидкостей і прискорень руху штовхача за рахунок можливості знайти дані у початкових і кінцевих точках графіка, що не було можливим при використанні традиційної методики.

Практична значимість. Розроблена методика автоматизованого проєктування робочих поверхонь розподільчих валів усіх типів із забезпеченням надійності й довговічності їх роботи.

Ключові слова: *двигун внутрішнього згоряння, розподільний вал, штовхач, кулачок, дискретне диференціювання, розділені різниці*

The manuscript was submitted 21.01.24.